Neuroscience Letters 630 (2016) 93–100

Contents lists available at ScienceDirect

Neuroscience Letters

journal homepage: www.elsevier.com/locate/neulet

Research article

An experimental study of the neurophysical mechanisms of photophobia induced by subarachnoid hemorrhage

Nazan Aydin[a], Dilcan Kotan[b,*], Sadullah Keles[c], Osman Ondas[d], Mehmet Dumlu Aydin[e], Orhan Baykal[c], Betul Gundogdu[f]

[a] Department of Psychiatry, Bakirkoy Mazhar Osman Education Hospital, Istanbul, Turkey
[b] Department of Neurology, Sakarya Universty School of Medicine, Sakarya, Turkey
[c] Department of Ophthalmology, Ataturk Universty School of Medicine, Erzurum, Turkey
[d] Opthalmology Clinic of Tokat-Erbaa Satate Hospital, Tokat, Turkey
[e] Department of Neurosurgery, Ataturk Universty School of Medicine, Erzurum, Turkey
[f] Department of Pathology, Ataturk Universty School of Medicine, Erzurum, Turkey

HIGHLIGHTS

- In our previous studies, we have reported that the parasympathetic preganglionic denervation of the CG can occur in patients with SAH or meningitis as the result of an arterial rupture in the subarachnoid space.
- The purpose of this study was to investigate the potential relationship between SAH-induced neuronal degeneration in the CG, pupil diameters and photophobia scores in rabbits.
- In our previous studies in SAH animal models, we studied the relationship between the neuronal density in the autonomic ganglia of cranial nerves and vasospasm in the cerebral arteries.
- This study could contribute to a better understanding of the pathways involved in SAH-induced photophobia.

ARTICLE INFO

Article history:
Received 29 March 2016
Received in revised form 28 April 2016
Accepted 11 July 2016
Available online 18 July 2016

Keywords:
Photophobia
Subarachnoid hemorrhage
Ciliary ganglion
Rabbit
Vasospasm

ABSTRACT

Background: Photophobia is defined as a painful psychosomatic discomfort triggered by intense light flow through the pupils to the brain, but the exact mechanism through which photophobia is induced by subarachnoid hemorrhage (SAH) is not well understood. In this study, we aimed to investigate whether there was any relationship between the mydriasis induced by the degeneration of the ciliary ganglion (CG) and photophobia in instances of SAH.
Materials and methods: Five of a total of 25 rabbits were used as the intact control group; five were used in the sham-operated control group; and the remaining 15 were used as the SAH group, which was created by injecting autologous blood into their cisterna magna. All animals were examined daily for 20 days to evaluate their level of photophobia, after which their brains, CGs and superior cervical ganglia (SCGs) were extracted bilaterally. The densities of normal and degenerated neurons in these ganglia were examined by stereological methods.
Results: In SAH animals with a high photophobia score, the mean pupil diameter and density of degenerated neurons density in the CG were greater than in cases with a low photophobia score ($p < 0.05$). Further analysis revealed that the increase in the density of degenerated neurons in the CG following SAH resulted in the paralysis of the parasympathetic pathway of the pupillary muscles and mydriasis, which facilitates the excessive transfer of light to the brain and photophobia.
Conclusion: Our findings indicate that SAH results in a high density of degenerated neurons in the CG, which induces mydriasis and is an important factor in the onset of photophobia. This phenomenon is likely due to more light energy being transferred through mydriatic pupils to the brain, resulting in vasospasm of the supplying arteries.

1. Introduction

The pupils play a critical role in transmitting light between the outside world to the brain. The quality of images is optimized by the

* Corresponding author.
E-mail address: dilcankotan@yahoo.com (D. Kotan).

http://dx.doi.org/10.1016/j.neulet.2016.07.013
0304-3940/

pupillary light reflex, in which the pupil constricts when the light intensity increases and pupil dilates when light intensity decreases. The photoreceptor cells of the retina include the rods, which are specialized for black and white vision in low light, and the cones, which are specialized for color vision in bright light [1]. The retinal ganglion cells projecting to the olivary pretectal nucleus also include a major projection to the Edinger-Westphal (EW) nucleus, which exerts parasympathetic action on the iris musculature via the ciliary ganglion (CG) [2]. The majority of the parasympathetic preganglionic motor neurons originating from the EW nucleus reach the CG via the oculomotor nerve (CN3), while a few reach the CG via the trigeminal nerve [2]. The terminal motor neurons of the pupils are located in the CG [3]. Anatomically, the CG is a small ganglion that is less than 2 mm long and resides within fat-filled connective tissue in the posterior orbit, just anterior to the superior orbital fissure. In humans, the CG contains an average of 3000 neurons and has a diameter of 20–35 μm., and the neurons in the CG primarily mediate pupilloconstriction and accommodation via the ciliary muscles [4].

Photophobia is a major symptom following subarachnoid hemorrhage (SAH) and is observed in many ophthalmic and neurologic disorders in response to intense light. Regardless of the cause, specific activation patterns in the trigeminal system can be observed in the trigeminal ganglion, trigeminal nucleus caudalis, ventroposteromedial thalamus, and anterior cingulate cortex during photophobia [5]. In 1996, Chronicle and Mulleners [6] speculated that the afferents from retinal ganglion cells that innervate the posterior thalamus and visual cortex along with sympathetic system hyperactivity might be responsible for photophobia. Clinically, it is widely known that light can initiate pain sensations in the orbit and head, whereas bright lights can also lead to trigeminal stimulation that produces oculocephalic discomfort that varies from mild to intolerable pain [7]. Recently, it has been reported that bright light significantly increases both the frequency and amplitude of the blinking reflex in subjects with photophobia [8].

In our previous studies, we have reported that the parasympathetic preganglionic denervation of the CG can occur in patients with SAH or meningitis as the result of an arterial rupture in the subarachnoid space. This denervation results in the degeneration of CG neurons followed by a dilated pupil [9,10]. Based on our current knowledge, we hypothesized that this loss of parasympathetic innervation in patients with SAH would lead to a relative sympathetic hyperactivity and thus an increased influx of light to the eye due to the resulting pupil dilation.

2. Material and methods–

This study was conducted on a total of 25 New Zealand white rabbits. The animal protocols were approved by Atatürk University Ethics Committee, and the care of the animals and the experiments were conducted according to the guidelines set forth by the same ethics committee.

2.1. Experimental protocol

Pupil diameters were measured in all animals in light and dark environments with an ocular coherence tomography device (Pentacam 70700: Oculus, Wetzlar, Germany), and fundoscopic examinations were performed for three times a day for two days prior to inducing SAH. The light sensitivity of the animals with dilated pupils was evaluated in a single-blind fashion by one of the researchers (M.D.A.) using a modified photophobia scoring system with grades from 0 to 3 (0 = normal, 1 = mild, 2 = moderate, 3 = severe) [11], and the mean values were used in the statistical analysis.

Five animals were used as the intact control group for the anatomical and histopathological examinations of the CGs, the SCGs, the CN3s, the posterior communicating arteries (PCoA) and the brainstem. All animals were anesthetized by isoflurane administered through a face mask, followed by a subcutaneous injection of 0.2 mL/kg of the anesthetic combination (ketamine HCl, 150 mg/1.5 mL; xylazine HCl, 30 mg/1.5 mL; and distilled water, 1 mL) before surgery. During the procedure, a dose of 0.1 mL/kg of the anesthetic combination was used when required; balanced, injectable anesthetics were used to reduce pain and mortality. Autologous blood (1 mL) was taken from the auricular vein and injected over the course of 1 min into the cisterna magna of animals in the SAH group using a 22-gauge needle. In the sham-operated control group, 1 mL of physiological serum was injected into the cisterna magna. The animals in the control group were not subjected to any injections. The animals were followed for 20 days without any medical treatment while their photophobia scores were recorded daily and then the animals were sacrificed. The brains, eyes and superior cervical ganglions (SCGs) of all animals were extracted and stored in 10% formalin solutions for histopathological examination.

2.2. Pupillary light reflex measurements

The measurement of pupil diameter, called pupillometry, was performed on unanesthetized rabbits using an ocular coherence tomography device as described below in detail [Fig. 1]. The animals were adapted to the experimental protocol by daily testing for one week to reduce stress-related pupil responses. The recordings were conducted during the middle of the light period, Zeitgeber Time (ZT) 6-6.5. Following a period of dark-adaptation for at least 1 h, rabbits were held carefully by the loose skin at the back of their neck to minimize blinking activity, which could interfere with the recordings; to immobilize the animal while ensuring unimpaired respiration; and to ensure a feeling of safety and facilitate a relaxed state. The rabbits were then positioned with one eye opposed to the outlet of an integrating sphere. The sphere was created from a 15-cm diameter white plastic ball, and to prevent light from escaping and thus interfering with the night goggles, the ball was painted black on the outside. The eye was recorded with an infrared sensitive camera (model XLVM, DAGE-MTI, Michigan City, IN, USA) fitted with a zoom lens (18–108-mm F2.5, Olympus, Tokyo, Japan) coupled to the opposite side of the sphere. The sphere was constantly illuminated by infrared light from diodes mounted in the bottom of the sphere. The camera was connected to a computer and operated by Streampix software (Norpix, Montreal, Canada). Light stimuli were provided by a 100-W halogen lamp and transmitted along a quartz fiber optic coupled to a circle surrounding the camera outlet, which illuminated the entire eye (Volpi AG, Schlieren, Switzerland). The intensity of the light was regulated with a set of glass neutral density filters (Chroma, Bellows Falls, VT, USA), and irradiance measures ($\mu W/cm^2$) were adjusted with a calibrated VEGA laser power meter (Ophir, Jerusalem, Israel). The eye was digitally captured at a frequency of 10 images per second for 2 min, and the pupil diameter was measured using ImageJ software (vers. 1.42q, NIH, USA) and converted to area. To correct for individual variation, data were normalized to the dark-adapted pupil size. Our preliminary experiments revealed that the non-invasive measurement of pupil diameter using ocular coherence tomography can reveal the constriction or dilation of the pupil, called miosis and mydriasis, respectively, in rabbits [Fig. 2].

2.3. Anatomical examination

Morphological examinations of the brains showed that all PCoAs were localized to the superomedial sides of the sulcus of the CN3 and extended from the fusion point of the internal carotid arter-

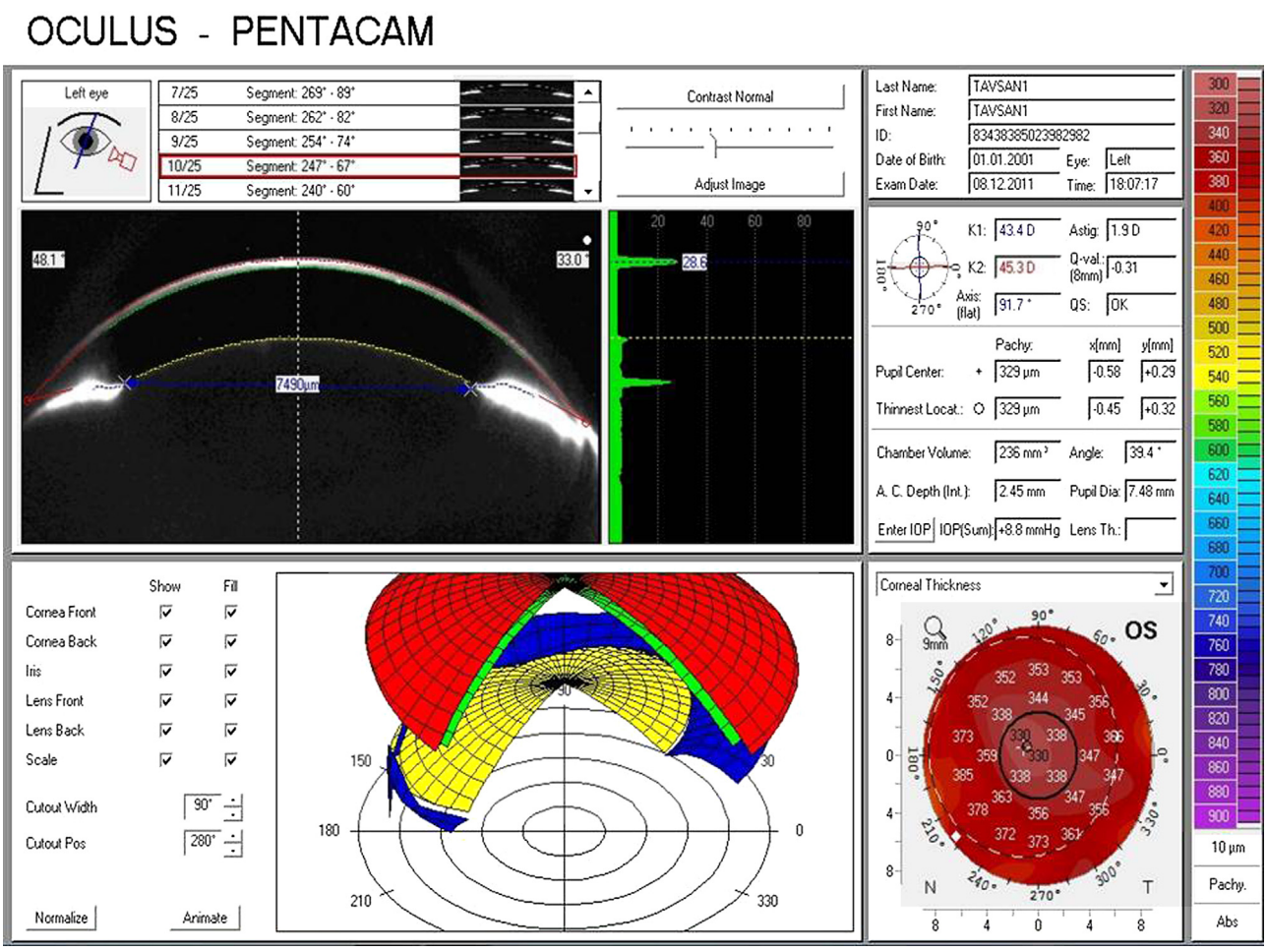

Fig. 1. Pupil diameters were measured using ophthalmic tomography as shown.

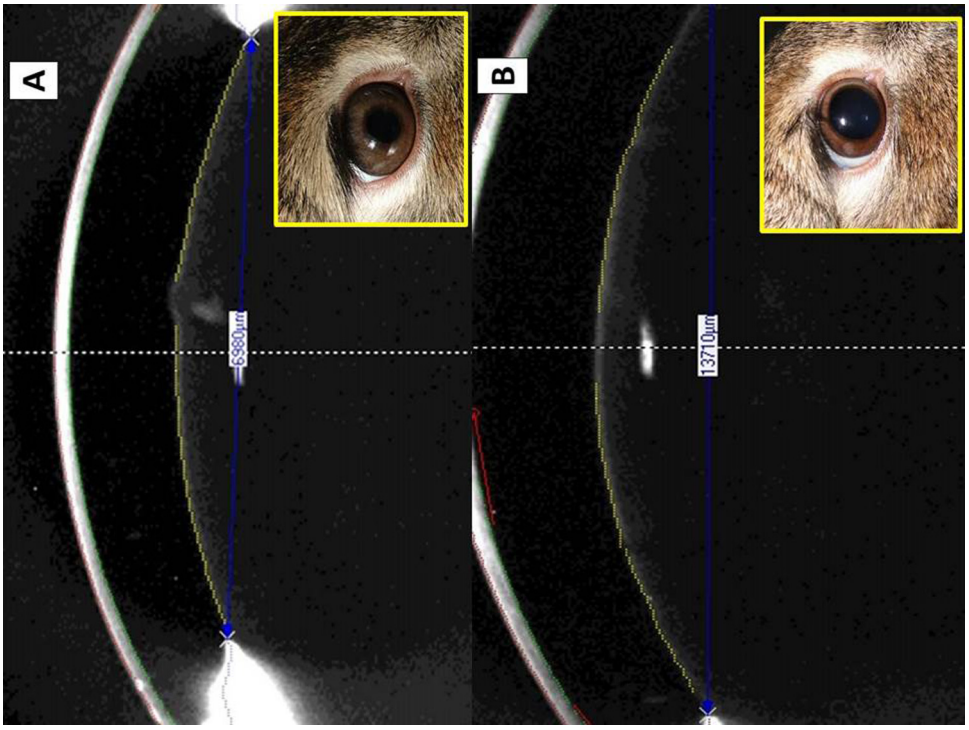

Fig. 2. Representative examples of miotic (decrease in size) (A) and mydriatic (increase in size) (B) pupils are shown.

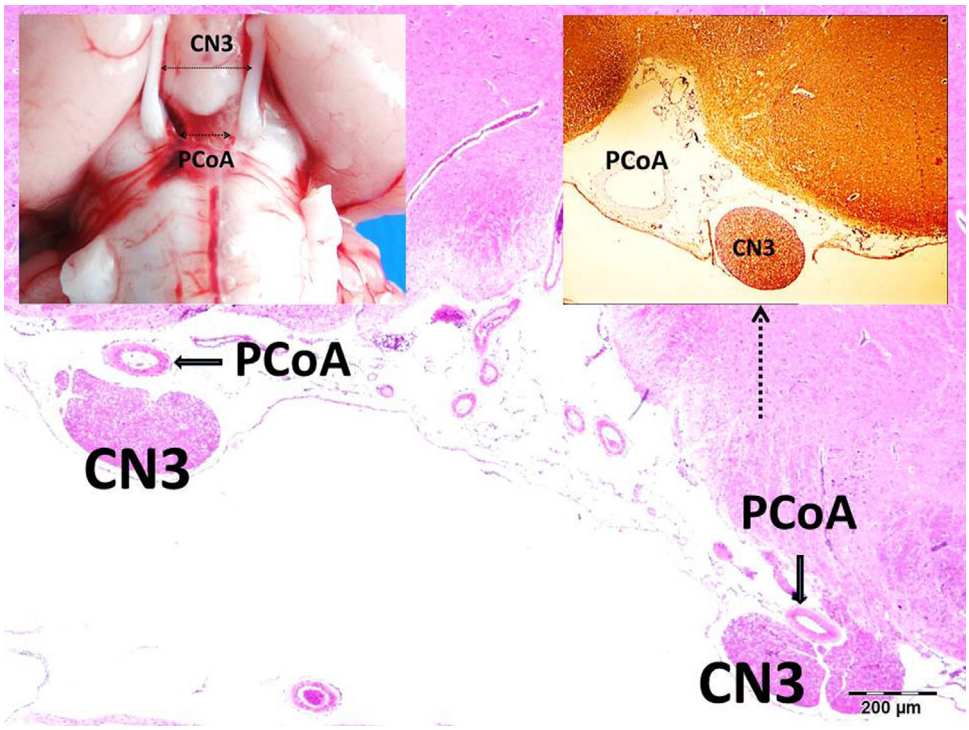

Fig. 3. Gross anatomical localization of the posterior communicating arteries (PCoA) and the oculomotor nerves (CN3) are shown in the left upper corner. The histopathological appearances of the PCoAs (arrows) and the CN3s are visible at the base (H&E, x20), and a higher magnification is shown in the right upper corner of photomicrograph (S-100, x40).

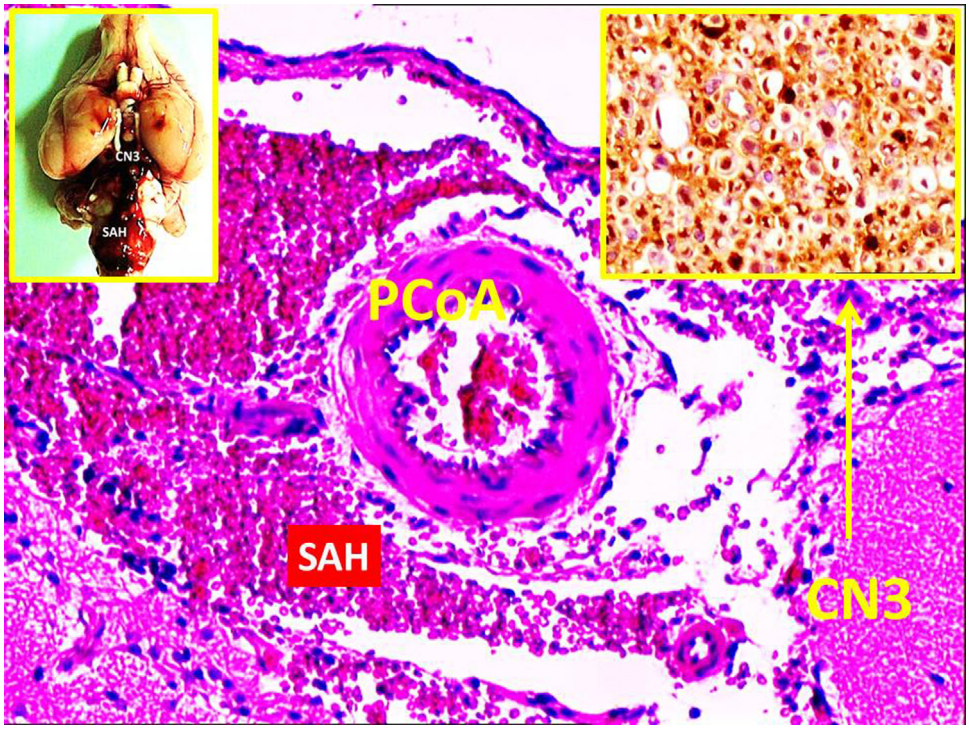

Fig. 4. Gross anatomical localization of the posterior communicating arteries (PCoA), the oculomotor nerves (CN3) in a rabbit with SAH are shown in the left upper corner, and a higher magnification is shown in the right upper corner (S-100, x40). The histopathological appearances of the PCoAs and the CN3s are visible at the base (H&E, x40).

ies and the origin of the posterior cerebral arteries [left corner in Fig. 3]. In animals with SAH, the lengths and external diameters of the arteries were reduced and their convolutions were increased with arachnoid thickenings and pia-arachnoid adhesions [left corner in Fig. 4]. The CGs were found to be embedded in loose fat tissue and to lay between the optic nerve and the lateral rectus muscle lateral to the ophthalmic artery. The CG connects to the ciliary nerves with a few fine branches. The parasympathetic root, derived from the EW nucleus, synapses in the CG, and the postganglionic fibers

travel along the short ciliary nerves to the sphincter pupilla and ciliary muscles.

2.4. Histopathological examination

All brains were horizontally sectioned at 2-mm distances from the origins of the CN3 s and embedded in paraffin blocks to observe the PCoAs and the CN3s. To estimate the neuronal density of the CG, the entire CG and its extensions were longitudinally embedded in paraffin blocks to visualize all of the roots. The tissues were stained with H&E and S-100 protein dyes, and the Cavalieri method was used to evaluate the density of the CG. The advantages of this method are that it easily estimates the particle number; can be readily performed; is intuitively simple; is free from assumptions about particle shape, size and orientation; and is unaffected by protection and truncation.

The physical dissector method was used to evaluate the numbers of living and degenerated neurons in the CG using observations such as cytoplasmic condensation, nuclear shrinking, cellular angulations and peri-cytoplasmic halo formation. This method easily estimates the particle number; can be readily performed; is intuitively simple; is free from assumptions about particle shape, size and orientation; and is unaffected by overestimation errors of neuronal numbers in the CG or by truncation. Two consecutive sections (dissector pairs) that were obtained from reference tissue samples were mounted on each slide. The paired reference sections were reversed to double the number of dissector pairs without having to cut new sections. The mean numerical density of the CG (Nv/Gv) per mm^3 was estimated using the following formula:

$$Nv/Gv = \Sigma Q^{-} / \Sigma Axd$$

Where ΣQ-N is the total number of counted neurons appearing only in the reference sections, d is the section thickness, and A is the area of the counting frame. The most effective way to estimate ΣA for the set of dissectors is via the formula ΣA = ΣP.a, where ΣP is the total number of counting set frames points and a is a constant area associated set point [12]. A and B are the areas of the counting frames [Fig. 5]. The Cavalieri volume estimation method was used to obtain the total number of neurons in each specimen, which were calculated by multiplying the volume (mm^3) by the numerical density of neurons in each CG. The numbers of normal and degenerated neurons in the CGs of each animal were counted. Histologically, cellular angulation, nuclear shrinkage, cytoplasmic condensation and cellular darkening were accepted as criteria for neuronal degeneration.

2.5. Statistical analysis

All values are expressed as the mean ± SD. The differences between the photophobia scores and the densities of degenerated neurons in the CGs were compared statistically. A one-way analysis of variance (ANOVA) followed by Boneferroni's post hoc test was used to determine significant differences between the groups for physiological parameters, pupil diameter and density of degenerated neurons in the CG. Because the total photophobia score data did not conform to a normal distribution, we used the Mann-Whitney U nonparametric test for statistical comparisons. Differences were considered to be significant at $p < 0.05$.

3. Results

In this study, four animals in the experimental SAH group died, while the others survived to complete the experiment. Of the animals in the intact control group, the pulse rate was 250 ± 30 beats/min, the respiration rate was 30 ± 7 breaths/min and the arterial oxygen saturation was 98 ± 5% (Table 1). However, during the early phase of SAH the heart rate decreased to 140 ± 40 beats/min, the breathing rate was 15 ± 5 breaths/min, and the oxygen saturation was 83 ± 10% (Table 1). During the late phase of SAH, the pulse rate increased to 330 ± 30 beats/min (Table 1), while the respiration rate increased to 40 ± 9 breaths/min with severe tachypneic and apneic variabilities (Table 1). Various electrocardiographic changes such as ST depression, ventricular extrasystols, bigeminal pulses, QRS separation, and fibrillations were observed in animals with SAH. In our further analyses of respiratory parameters, a decrease in respiration frequency (bradypnea) and an increase in respiration amplitude (30%) were observed during the first hours of SAH. Finally, increased frequency of respiration (tachypnea), decreased respiration amplitude (30 ± 8%), shortening of inspiration with prolonged expiration time, apnea-tachypnea attack, diaphragmatic breath and respiratory arrest were observed in animals with fatal SAH. The differences between the groups in terms of pulse rate, respiration rate and oxygen saturation, except for between intact control and sham-operated groups, were statistically significant ($p < 0.05$).

Table 1
Physiological parameters of rabbits in different groups.

	Intact control (n = 5)*	Sham-operated (n = 5)*	Early phase of SAH (n = 15)*	Late phase of SAH (n = 11)*
Pulse rate (beats/min)	250 ± 30	205 ± 22	140 ± 40	330 ± 30
Respiration rate (breaths/min)	30 ± 7	24 ± 5	15 ± 5	40 ± 9
Oxygen saturation (%)	98 ± 5	93 ± 8	83 ± 10	68 ± 9

* All values are expressed as the mean ± standard deviation. Significant differences were observed between groups, except between the intact control and sham-operated groups ($p<0.05$).

A representative macroscopic appearance of the brain, the CN3 and the PComA of a normal animal is illustrated in Fig. 3, while those of an animal with SAH are shown in Fig. 4. In histopathological examination of the CN3, axonal and periaxonal thinning, axonal loss and expanded interaxonal space were accepted as axonal degeneration criteria. The changes in the CN3 were observed more often in animals with fatal SAH [Fig. 4] than in animals that survived [Fig. 3].

The four animals that died during the study showed normal SCGs. The mean normal neuronal density of the CGs was 3310 ± 930 neurons/mm^3. The pupil diameters, the mean density of degenerated neurons and the total photophobia scores of animals in the SAH group were significantly greater than of those in the control and sham-operated groups ($p < 0.001$, $p < 0.001$ and $p < 0.005$, respectively). The mean values of pupil diameter, density of degenerated neurons in the CG, and total photophobia score are shown in Table 2.

The mean pupil diameter, density of degenerated neurons in the CG, and total photophobia score in animals within the SAH group that had a high photophobia score were greater than those SAH animals with a low photophobia score ($p = 0.016$, $p = 0.017$ and $p = 0.003$, respectively). The mean values of pupil diameter, density of degenerated neurons in the CG, and total photophobia score are shown in Table 3.

Our findings suggest that ischemia in the CN3 of the brainstem resulting from vasospasm of the supplying arteries and the high density of degenerated neurons in the CG might play major roles in the development of mydriasis in animals with SAH. Importantly, photophobia scores were found to be higher in animals showing greater levels of vasospasm in the PCoA and a higher density of degenerated neurons in the CG (data not shown). Accordingly, both the density of degenerated axons in the CN3 and the density of degenerated neurons in the CG increased more in animals with severe vasospasm in the PCoA compared to those with less severe vasospasm (data not shown).

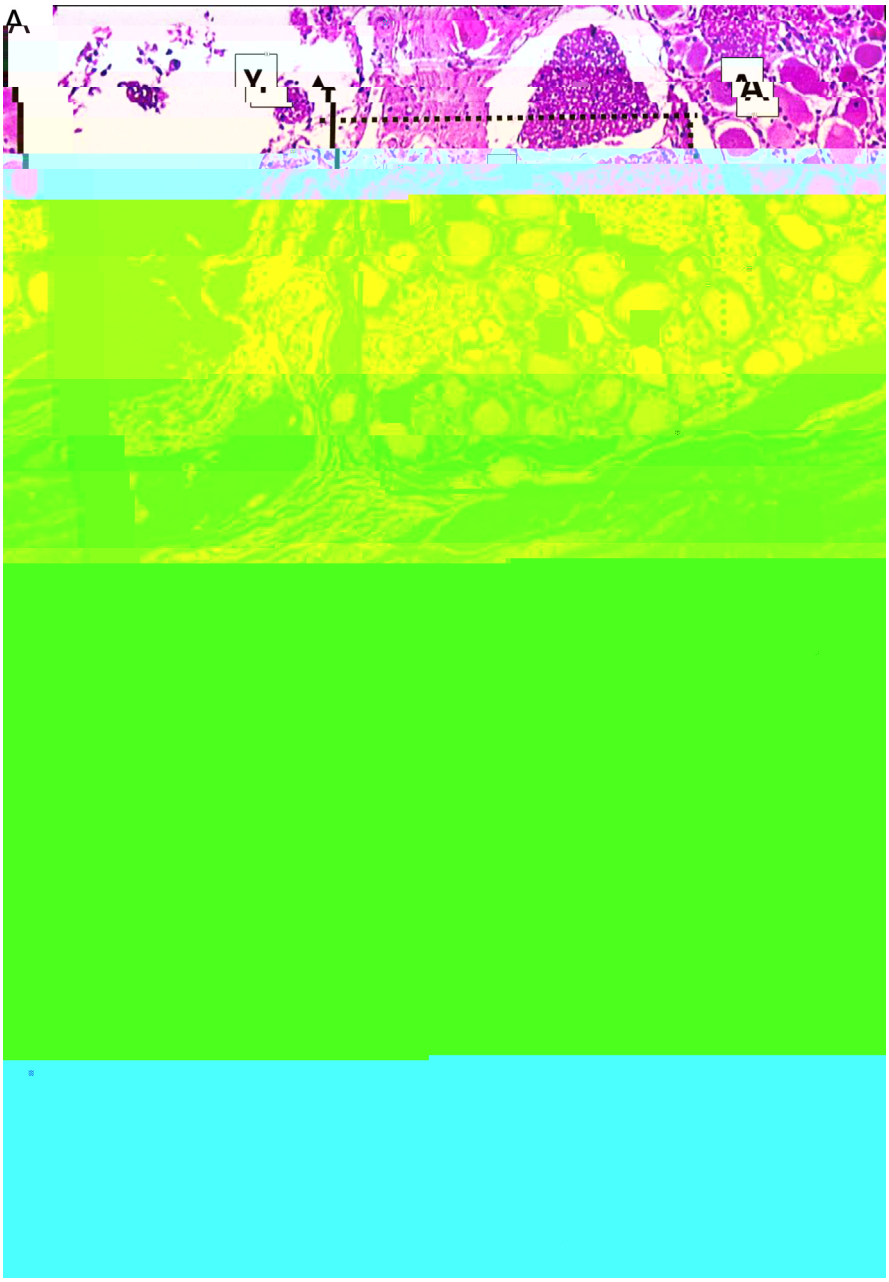

Fig. 5. Stereological cell counts of the ciliary ganglia (CG) in a rabbit. Application of the physical dissector method in which micrographs in the same fields of view (A, B) were taken from two parallel, adjacent thin sections separated by a distance of 5 μm. The upper and right lines in the unbiased counting frames represent the inclusion lines, and the lower and left lines, including the extensions, are exclusion lines. The neuronal nuclei touching the inclusion lines were excluded, and the nuclei profiles touching the inclusion lines and located inside the frame were counted as dissector particles unless their profile extended up to the reference section. The number of neurons from the two dissectors within a given volume were calculated as the product between the counting frame area and the distance between the sections. The numerical density of the neurons in the CG is calculated as NvGN = ΣQ⁻GN/txA. In this application, the nuclei marked with '1,2,5′ are dissector particles in A. Section B shows them as they disappeared. The nuclei marked with '3,4,6-8′ are not a dissector particle in A. Section B shows '3,4,6-8′ as it disappeared (H&E, 40, *N* normal; *D* degenerated).

4. Discussion

The purpose of this study was to investigate the potential relationship between SAH-induced neuronal degeneration in the CG, pupil diameters and photophobia scores in rabbits. Based on the findings of this and our previous studies, we suggest that ischemic neurodegeneration in the CG developed due to vasospasms in the PCoA, which results in mydriatic pupils due to parasympathetic insufficiency, excessive light influx to the brain, and photophobia.

Pupils regulate the amount, quality and quantity of visual information by changing their diameters in response to light. This pupil light reflex is important for the maintenance of vision quality and for protecting the brain from the hazardous effects of light [13]. The pupillary light reflex is under the control of retinal ganglion cells that project to the olivary pretectal nucleus, which has a major projection to the EW nucleus that exerts its parasympathetic action on the iris musculature via the CG [2]. Anatomically, the EW nucleus receives pretectal inputs for the pupillary light reflex that synapse on preganglionic motor neurons that control the lens and pupil [2]. The sphincter muscle is innervated by postganglionic parasympathetic fibers of the CG that are controlled by the preganglionic fibers originating from the EW nucleus in the midbrain. The motor neurons of pupils are located in the CG and project to the ciliary muscles via short ciliary nerves [3,4]. Most of the preganglionic motor neu-

Table 2
Pupil diameters, densities of degenerated neurons in the CG, and total photophobia scores of rabbits from different groups.

	Intact control (n = 5)	Sham-operated (n = 5)	SAH (n = 11)	*p*
Pupil diameter (μm)	6980 ± 540	9080 ± 1230	13710 ± 2140	0.267 for Group 1–2 <0.001 for Group 1–3 <0.001 for Group 2–3
Density of degenerated neurons in the CG (n/mm^3)	5 ± 2	79 ± 12	1370 ± 450	0.736 for Group 1–2 <0.001 for Group 1–3 <0.001 for Group 2–3
Total photophobia score	0.2 ± 0.5	0.4 ± 0.6	1.7 ± 1.2	0.690 for Group 1–2 <0.005 for Group 1–3 <0.006 for Group 2–3

CG ciliary ganglion; *SAH* subarachnoid hemorrhage. All values are expressed as mean ± standard deviation.

Table 3
Comparison of the pupil diameters and densities of degenerated neuron in the CG with photophobia score of rabbits in the SAH group.

	SAH with low photophobia score (n = 6)*	SAH with high photophobia score (n = 5)*	*p*
Pupil diameter (μm)	10080 ± 1940	13710 ± 2140	0.016
Density of degenerated neurons in the CG (n/mm^3)	1060 ± 220	1840 ± 610	0.017
Total photophobia score	0.8 ± 0.4	2.8 ± 0.5	0.003

CG ciliary ganglion; *SAH* subarachnoid hemorrhage. All values are expressed as the mean ± standard deviation.

* In each animal, photophobia score values such as 0 and 1 were accepted as "low", while the values such as 2 and 3 as "high&rdquo.

rons originating from the EW nucleus reach the CG via CN3, while some reach the CG via the long ciliary fibers of the trigeminal nerve [2].

The neurons of the CG mediate pupilloconstriction and accommodation on ciliary muscles [14]. Pupilloconstriction is achieved by the simultaneous contraction of the iris sphincter muscle and the relaxation of the iris dilator muscles [15]. Preganglionic sympathetic fibers arising from the intermediolateral cell column of Th1-2 spinal cord travel to the SCG, and postganglionic sympathetic fibers follow the internal carotid artery and pass through the cavernous sinus by joining the ophthalmic branch of the trigeminal nerve, innervating the iris dilator muscles [16]. In animals, unilateral lesions of the EW nucleus abolish the pupillary light reflex in the eye contralateral to the lesion [17]. The bilateral destruction of the EW nucleus leads to loss of the light reflex and impaired visual acuity [18]. Jackson [19] reported that lesions of the preganglionic axons of the CG, such as neonatal optic nerve section, cause the degeneration of the CG cells in the rabbit.

Clinically, pupillary dysfunction occurs in patients with diabetes mellitus, Holmes-Adie syndrome, the Argyll Robertson pupil, paraneoplastic syndrome, and high intraocular pressure [20]. Episodic unilateral mydriasis is likely the result of parasympathetic hypofunction in the iris sphincter or sympathetic hyperactivity of the iris dilator in patients with migraine [21]. Acute unilateral mydriasis with complete palsy of CN3 is a classical presentation of PCoA aneurysm [22]. Moreover, mydriasis can be associated with trigeminocorneal reflex dysfunction on cardiac and pupillary sympathetic imbalance in episodic cluster headache [23].

Today, there is little knowledge regarding the pathophysiology of photophobia, although the following mechanisms have been suggested: enhancement of light inputs from the visual cortex to the trigeminal system [6]; irritation of trigeminal nerve nociceptors that innervate the eye, consequently activating the spinal trigeminal nucleus, midbrain and thalamus [24]; hyperactivity of the sympathetic system[25]; irritation of the basal meninges around the diaphragma sellae [26]; and hypersensitivity of the visual cortex [26]. In the presence of bright light, rats exhibit blink modifications similar to those of people experiencing

ulation of the CG could constitute a new therapeutic modality for treating vasospasm-related photophobia following SAH [37].

This study could contribute to a better understanding of the pathways involved in SAH-induced photophobia. Rabbits were chosen for this study because the rabbit SAH model has a steady time course of cerebral vasospasm, usually beginning on the third day [38]. Nevertheless, we recognize several limitations of the current study that need to be addressed. First, the anatomy of the encephalic vasculature and the CG in animals differs from that in humans. Second, there is a discrepancy in the time course of vasospasm following the onset of SAH between animals and humans. Third, another weakness of animal SAH models using the direct injection of blood into the cisterna magna is a failure to reproduce the mechanical trauma, which is the first insult upon the cerebral vasculature following aneurysm rupture in humans [39]. An ideal animal model should be representative of human SAH; unfortunately, not all large animal experimental models have human relevance and validity, and species-related differences should be regarded before interpreting the data.

5. Conclusion

From a theoretical point of view, it is expected that the miotic potential of the CG would be diminished by degeneration of the neurons in the CG. It is well known that pupilloconstrictor molecules are synthesized by neurons in the CG and are secreted from nerve terminals at the end of sphincter muscle terminals that produce miotic pupils. As a result, we speculate that decreased neuronal numbers might result in a deficiency in pupilloconstrictor chemicals in the CG and cause photophobia in normal patients. Thus, these mechanisms would subsequently increase the severity of photophobia in cases of SAH. For this reason, new approaches toward improving cerebral blood flow and the regulation of the light reflex should be investigated.

Disclosure

Authors declare no conflict of interest.

Acknowledgment

No.

References

[1] L.M. Tessier, in: E.R. Cadel, J.R. Schwardz (Eds.), Photoconduction and Information Processing in Retina.) Principles of Neural Science, Elsevier, New York, 1991, pp. 441–466.
[2] T. Kozicz, J.C. Bittencourt, P.J. May, A. Reiner, P.D. Gamlin, M. Palkovits, et al., The Edinger-Westphal nucleus: a historical, structural, and functional perspective on a dichotomous terminology, J. Comp. Neurol. 519 (2011) 1413–1434.
[3] S. Kuchiiwa, T. Kuchiiwa, S. Nakagawwa, M. Ushikawa, Oculomotor parasympathetic pathway to the accessory cilary ganglion by passing the main ciliary ganglion by way of the trigeminal nerve, Neurosci. Res. 18 (1993) 79–82.
[4] G.M. Perez, R.B. Keyzer, Cell body counts in human ciliary ganglia, Invest. Ophthalmol. Vis. Sci. 27 (1986) 1428–1431.
[5] E.A. Moulton, L. Becerra, D. Borsook, An fMRI case report of photophobia: activation of the trigeminal nociceptive pathway, Pain 145 (2009) 358–363.
[6] E.P. Chronicle, W.M. Mulleners, Visual system dysfunction in migraine: a review of clinical and psychophysical findings, Cephalalgia 16 (1996) 525–535.
[7] L.M. Cruz-Orive, E.R. Weibel, Recent stereological methods for cell biology: a brief survey, Am. J. Physiol. 258 (1990) L148–L156.
[8] S. Dolgonos, H. Ayyala, C. Evinger, Light-induced trigeminal sensitization without central visual pathways: another mechanism for photophobia, Invest. Ophthalmol. Vis. Sci. 52 (2011) 7852–7858.
[9] M.D. Aydin, I. Akyol-Salman, O. Sahin, Histopathological changes in ciliary ganglion of rabbits with subarachnoid hemorrhage, Int. J. Neurosci. 115 (2005) 1595–1602.
[10] M.D. Aydin, S. Onder, H. Ulvi, A. Onder, O. Baykal, Histopathological alterations in ciliary ganglions in meningitis: an experimental study, Minim. Invasive Neurosurg. 48 (2005) 297–301.
[11] W.G. Stroop, D.C. Schaefer, Severity of experimentally reactivated herpetic eye disease is related to the neurovirulence of the latent virus, Invest. Ophthalmol. Vis. Sci. 28 (1987) 229–237.
[12] D.C. Sterio, The unbiased estimation of number and sizes of arbitrary particles using the dissector, J. Microsc. 134 (1984) 127–136.
[13] B.K. Ahlborn, Ligt, abundant information, in: B.K. Ahlborn (Ed.), Zoological Physics. Quantitative Models of Body Design, Actions, and Physical Limitations of Animals, Springer-Verlag Berlin Heidelberg, New York, 2006, pp. 261–307.
[14] W. Kirch, W. Neuhuber, E.R. Tamm, Immunohistochemical localisation of neuropeptides in human ciliary ganglion, Brain Res. 681 (1995) 229–234.
[15] R. Suzuki, T. Oso, S. Kobayashi, Cholinergic inhibitory response in the bovine iris dilalatatory muscle, Invest. Ophthalmol. Vis. Sci. 24 (1983) 760–765.
[16] G.W. Paulson, J.P. Kapp, Dilatation of the pupil in the cat via the oculomotor nerve, Arch. Ophthalmol. 77 (1967) 536–540.
[17] P.D. Gamlin, A. Reiner, J.T. Erichsen, H.J. Karten, D.H. Cohen, The neural substrate for the pupillary light reflex in the pigeon (Columba livia), J. Comp. Neurol. 226 (1984) 523–543.
[18] W. Hodos, R.F. Miller, M.M. Ghim, M.E. Fitzgerald, C. Toledo, A. Reiner, Visual acuity losses in pigeons with lesions of the nucleus of Edinger-Westphal that disrupt the adaptive regulation of choroidal blood flow, Vis. Neurosci. 15 (1998) 273–287.
[19] P.C. Jackson,